Early visualization of the irreversible electroporation ablated tissue margin by contrast enhanced imaging in rodent model

Y. Guo[1], Y. Zhang[1,2], G. Nijm[3], A. Sahakian[3], G-Y. Yang[4], R. Omary[1,5], and A. Larson[1,5]

[1]Department of Radiology, Northwestern University, Chicago, IL, United States, [2]Department of Bioengineering, University of Illinois at Chicago, Chicago, IL, United States, [3]Department of Electrical Engineering and Computer Science, Northwestern University, Evanston, IL, United States, [4]Department of Pathology, Northwestern University, Chicago, IL, United States, [5]Department of Biomedical Engineering, Northwestern University, Chicago, IL, United States

INTRODUCTION

Electroporation involves targeted delivery of electrical pulses to permeabilize cell membranes, either temporarily (reversible electroporation) or permanently (irreversible electroporation, IRE). IRE was introduced as a new tissue ablation technique in 2005. IRE uses targeted delivery of electrical pulses to induce tissue necrosis due to permanent cell membrane defects (1,2). Assessment of tissue response to IRE may be critical (3). For our study, we hypothesized that contrast enhanced MRI would permit early quantification of IRE ablation response. We demonstrate that contrast enhanced imaging can visualize the IRE ablated tissue margin (differentiating reversible / irreversible zones) to provide an accurate prediction of the ablated tissue region.

METHOD

Animal Model 17 adult male Sprague Dawley rats (weight 301-325g) were used for our ACUC-approved experiments. 15 rats underwent IRE ablation procedure with a pre-IRE injection of 8μL/g Gd-DTPA solution (Magnevist®; Berlex, Montville, NJ).2 control rats underwent IRE procedure without Gd-DTPA infusion. *MRI* All experiments were performed using a 3.0T clinical MR scanner (Magnetom Trio, Siemens Medical Solutions) with custom-built rodent receiver coil (Chenguang Medical Technologies Co., Shanghai, China). Before imaging, rats were anaesthetized with intra-peritoneal injection of ketamine (80mg/kg) and xylazine (10mg/kg). Following initial localization scans, contrast enhanced images were acquired at 2 hours interval post-IRE using T1-weighted gradient echo (T1-w GRE) sequence and segmented inversion-recovery turbo fast low-angle shot (IR-FLASH) sequence at identical coronal slice positions. T1-w GRE parameters: TR/TE = 200/2.68ms, FA = 90°, 2mm slices, Avg = 3, FOV = 70×150 mm2, matrix = 90×192, bandwidth = 500 Hz/pixel. IR turbo-FLASH parameters were: FA = 20° (others same with T1-GRE) with multiple inversion times (100 to 250ms). After imaging, rats were euthanized and livers harvested for histological evaluation. *IRE Procedures* A BTX Electroporator (ECM830; Harvard apparatus, Holliston, MA) function generator and a parallel two-needle array were used. Rat was fixed in a supine position with a mini-laparotomy incision performed to expose left hepatic lobe and insert IRE electrodes parameters were applied. The following IRE parameters were fixed in each rat: total number of pulses = 8, each pulse duration = 100 μs and the interval between two pulses = 100 ms; the variable parameters were: 1000 Voltage, 10mm spacing electrodes in Group 1, 500Voltage, 5mm spacing in Group 2 and 1000Voltage, 5mm spacing in Group 3-4). *Images Analysis* Image post-processing was performed using Matlab software. For images in Groups 1-3, regions of interest (ROIs) encompassing the anticipated IRE zone were manually drawn on both T1-w GRE and IR FLASH images (to compare with the ablated necrosis area measured on H&E slides one day later). *Histology* Each rat was euthanized 24 hours post-IRE. Liver specimens were fixed in formalin and paraffin embedded and H&E staining was performed. Histological slides were digitized using a multi-channel automated imaging system. The areas of the ablated necrotic tissue were measured based upon cell morphology. *Statistical Analysis* All statistics were performed using SPSS (SPSS, Chicago, IL, USA). The Spearman's correlation coefficient was calculated to assess the correlation between MRI-measured IRE zone (T1-w GRE and IR-FLASH, respectively) and area of ablated tissue on histological slides (mm^2). Test was considered statistically significant with a p-value < 0.05. Bland-Altman plots were generated to investigate the agreement between MRI-estimated IRE zone and the ablated area on H&E slides.

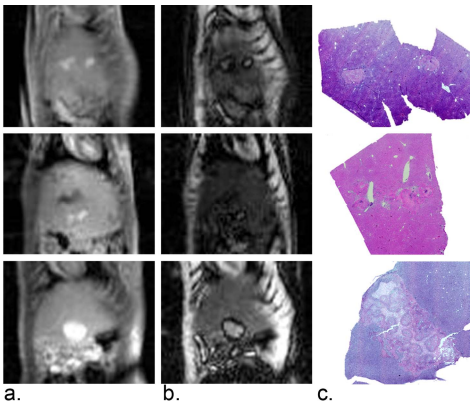

Fig. 1 T1-w GRE images (**a**), IR-FLASH images (**b**) and correlated H&E slides (**c**) (Group 1-3 shown in each row).

RESULTS

T1-w GRE and IR-FLASH images and corresponding histological slides are shown in **Fig. 1**. These lesions were consistently hyper-intense within T1-w GRE images (**Fig. 1a**). However, there were consistently two zones in those images with IRE time adjusted to null the SI of the reversible rim (reversibly electroporated penumbra); these included the hypo-intense reversible zone and central hyperintense irreversible zone (**Fig. 1b**). IR images with TI adjusted to null the SI of IRE zone (TI*ire*), reversible rim (TI*re*) and normal liver parenchyma (TI*nor*) were consistently TI*nor* > TI*re* > TI*ire*. Both T1-w GRE and IR-FLASH measured IRE zones were well correlated with the ablated necrosis area (r = 0.891, p<0.0001 and r = 0.939, p<0.0001, respectively) (**Fig. 2b**). However, the Bland-Altman plot indicated a bias for T1-w GRE measurements tending to predict a larger IRE ablation zone (**Fig. 2c**) but IR-FLASH images were more accurate (**Fig. 2d**).

CONCLUSION

Inversion recovery prepared contrast enhancement imaging, with IR time adjusted to null the signal intensity from the reversibly electroporated zone, can better delineate the IRE ablation region and provide more accurate prediction of the IRE ablation zone compared to T1-weighted GRE imaging. This technique can early detect tissue response to IRE ablation and might be helpful to guide further treatments.

Reference:

[1] Davalos RV et al. Ann Biomed Eng 2005;33(2):223-231.

[2] Rubinsky B et al. Technol Cancer Res Treat 2007;6(4):255-260.

[3] Gervais DA et al. Abdom Imaging 2009;34(5):593-609.

[4] Edd JF et al. Technol Cancer Res Treat 2007;6(4):275-286.

[5] Miklavcic D et al. Biochim Biophys Acta 2000;1523(1):73-83.

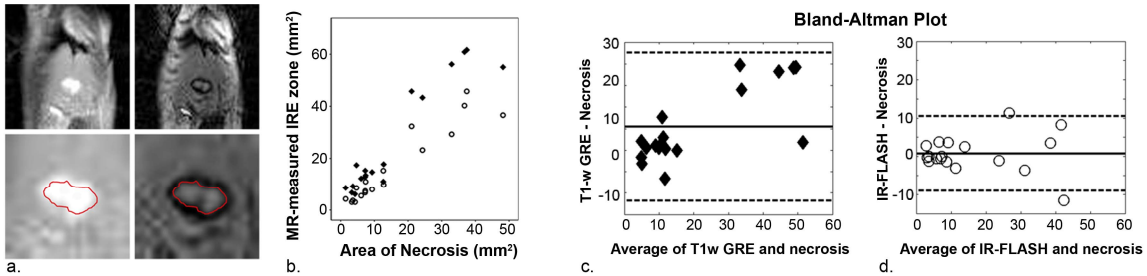

Fig. 2 Representative T1-w GRE and IR-FLASH images (**a**), correlation of MRI-measured IRE zones with ablated necrosis area (♦,T1-w GRE-measured IRE zone; ○, IR-FLASH measured IRE zone) (**b**) and Bland-Altman plot comparing T1-w GRE and IR-FLASH with ablated necrotic area (**c** and **d**, respectively).

Acknowledgements: The authors wish to acknowledge grant support from NIH CA134719 and NIH UL1 RR025741.